

# Effects of high-permittivity materials on absolute RF coil performance as a function of $B_0$ and object size

Riccardo Lattanzi<sup>1,2</sup>, Manushka V Vaidya<sup>1,2</sup>, Giuseppe Carluccio<sup>1</sup>, Daniel K Sodickson<sup>1,2</sup>, and Christopher M Collins<sup>1,2</sup>

<sup>1</sup>The Bernard and Irene Schwartz Center for Biomedical Imaging, Department of Radiology, New York University School of Medicine, New York, NY, United States,

<sup>2</sup>The Sackler Institute of Graduate Biomedical Sciences, New York University School of Medicine, New York, NY, United States

**TARGET AUDIENCE:** RF coil designers and anyone interested in analytic methods for rapid electromagnetic field simulation in MRI.

**PURPOSE:** The use of dielectric pads of high-permittivity material (HPM) has recently been proposed to improve transmit efficiency and signal-to-noise ratio (SNR) of radiofrequency (RF) coils (1-3). Previous studies have employed pads of HPM under (1-2) or next to (3) the coil elements of single-channel coils or small arrays to remove  $B_1^+$  inhomogeneities or increase SNR locally. We investigated the effect of a layer of HPM, placed between the conductors and the object, on the overall performance of a 32-element array enclosing a spherical object, using the ultimate intrinsic SNR (UISNR) as the reference. We compared the results for different values of the static magnetic field ( $B_0$ ) and different sizes of the object, varying the permittivity, thickness and position of the HPM layer.

**THEORY AND METHODS:** UISNR and the SNR of actual coil arrays surrounding a uniform sphere can be calculated by employing the dyadic Green's function (DGF) theory and a complete set of current modes, which are combined to define optimal current distributions at some distance from the object (4). We extended the formalism to the case of multi-layered spherical geometries (Fig. 1). We constructed the scattering DGF in each layer in terms of the spherical vector wave functions by applying the method of scattering superposition (5). UISNR and SNR calculations were performed for a homogenous sphere ( $\epsilon_r$  and  $\sigma$  of average brain tissue (4)) of various sizes (radius  $r_s = 6.4, 8.4$  and  $10.4$  cm), defining the current distribution at a distance of 2 cm ( $r_c = r_s + 2$  cm) from the surface of the object (Fig. 1). The intermediate space was divided into two equal layers ( $r_0 = r_s + 1$  cm) and we considered various cases: both layers empty ( $\epsilon_{rA}$  and  $\epsilon_{rB} = 1$ ), one of the two layers ( $\epsilon_{rA}$  or  $\epsilon_{rB} > 1$ ) or both layers ( $\epsilon_{rA}$  and  $\epsilon_{rB} > 1$ ) filled with HPM. Relative permittivity of the HPM was varied from 20 to 600. We simulated the absolute coil performance (i.e., SNR of the coil as a percentage of the UISNR) for a 32-element encircling loop array as a function of  $B_0$  and position within the sphere for a transverse field-of-view.

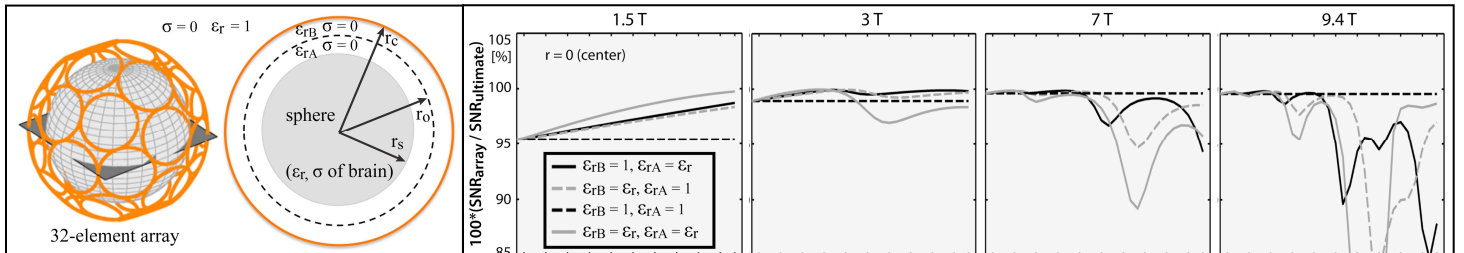


**Fig. 1. Schematic of the coil, the FOV and the multi-layer spherical geometry.** Both the ideal current distribution and the coil conductors were defined on a spherical surface at a 2 cm distance from the object.

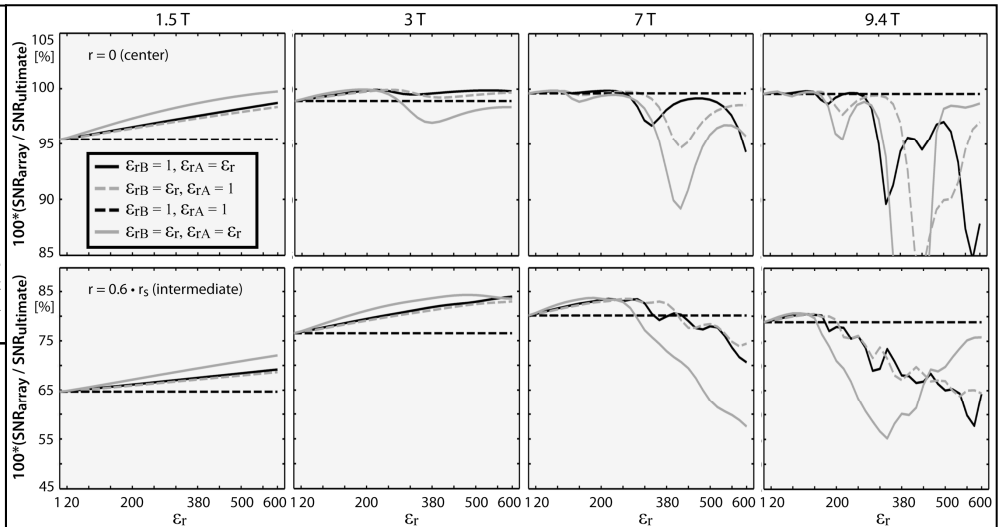


**Fig. 2. Absolute coil performance (% of UISNR) vs. relative permittivity of the HPM for a voxel in the center (top row) and at an intermediate position (bottom row).** Results are shown for the 8.4 cm radius sphere, various  $B_0$  and different configurations of the dielectric layer. At 1.5T and 3T, adding HPM allows approaching UISNR more closely. At ultra-high field, adding HPM is not beneficial in the center of the object and, due to wavelength effects, could decrease array performance.

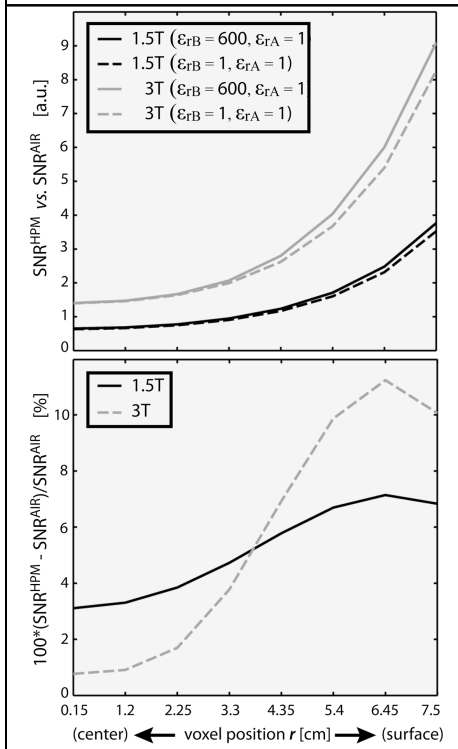


**Fig. 3. SNR benefit with a 1 cm layer of HPM below the coil elements of the 32-element array.** Results are shown for an 8.4 cm radius sphere as a function of position.

**RESULTS:** At low fields (Fig. 2), array SNR approaches the UISNR more closely if the space between the coil and the object is filled with HPM (gray line), or if a layer of HPM is added either below the coil (dotted gray line) or on top of the object (black line). Coil performance for an intermediate voxel (second row in Fig 2) increases from 75% to almost 85% of the optimum at 3T. At 7T and 9.4T, wavelength effects can reduce performance for high values of the relative permittivity. The patterns (not shown) for other object sizes are similar, with larger sphere radii producing effects comparable to higher  $B_0$ . Fig. 3 shows that the SNR advantage of adding a 1 cm layer of HPM underneath the coil conductors, arguably the most practical solution, is larger near the surface of the object.

**DISCUSSION AND CONCLUSION:** Our results showed that, although obtained with a different weighted combination of the basic current modes, UISNR does not change if a layer of HPM (with zero conductivity) is added between the object and current distribution. Therefore, the coil performance improvements shown in Fig. 2 are only due to the HPM. Coil noise and radiation losses were not included in the simulations. Adding coil noise would scale down all the curves in Fig. 2 equally. Adding radiation loss would amplify the advantages of HPM, as they improve matching (6) and therefore reduce radiation losses. Although we used a fully encircling array, it has been shown that SNR performance is not affected if the same number of coils are arranged to leave space where the neck and the face of a patient would be (7). The use of a simple geometry is a limitation, but nevertheless can provide physical insights useful for coil design (4). For example, Fig. 3 suggests that by simply adding a 1 cm layer of HPM in the coil substrate, SNR could increase by more than 5% on average at 1.5T and 3T. Future work will include cylindrical geometries (to approximate body imaging) and experimental validation.

**REFERENCES:** [1] QX Yang et al. MRM 2011; 65(2) p. 358. [2] P de Heer et al. MRM 2012; 68(4) p. 1317. [3] M Vaidya et al. ISMRM 2013, p. 4379. [4] R Lattanzi and DK Sodickson MRM 2012; 68(1) p. 286. [5] LW Li et al. IEEE Trans. Microw. Theory Tech. 1994; 42(12) p. 2302. [6] G Carluccio et al. ISMRM 2013, p. 4374. [7] R Lattanzi et al. NMR in Biomed 2010; 23(2) p. 142.